

Leakage currents mechanism in thin films of ferroelectric $\text{Hf}_{0.5}\text{Zr}_{0.5}\text{O}_2$

Damir R Islamov^{1,2}, A G Chernikova³, M G Kozodaev³, A M Markeev³, T V Perevalov^{1,2}, V A Gritsenko^{1,2} and O M Orlov⁴

¹ Rzhanov Institute of Semiconductor Physics SB RAS, Novosibirsk 630090, Russian Federation

² Novosibirsk State University, Novosibirsk 630090, Russian Federation

³ Moscow Institute of Physics and Technology, Dolgoprudniy 141700, Russian Federation

⁴ JSC Molecular Electronics Research Institute, Zelenograd, Moscow 124460, Russian Federation

E-mail: damir@isp.nsc.ru

Abstract. We study the charge transport mechanism in ferroelectric $\text{Hf}_{0.5}\text{Zr}_{0.5}\text{O}_2$ thin films. Transport properties of $\text{Hf}_{0.5}\text{Zr}_{0.5}\text{O}_2$ are described by phonon-assisted tunnelling between traps. Comparison with transport properties of amorphous $\text{Hf}_{0.5}\text{Zr}_{0.5}\text{O}_2$ demonstrates that the transport mechanism does not depend on the structure. The thermal and optical trap energies 1.25 eV and 2.5 eV, respectively, in $\text{Hf}_{0.5}\text{Zr}_{0.5}\text{O}_2$ were determined based on comparison of experimentally measured data on transport with simulations within phonon-assisted tunnelling between traps. We found that the trap density in ferroelectric $\text{Hf}_{0.5}\text{Zr}_{0.5}\text{O}_2$ is slightly less than one in amorphous $\text{Hf}_{0.5}\text{Zr}_{0.5}\text{O}_2$. A hypothesis that oxygen vacancies are responsible for the charge transport in $\text{Hf}_{0.5}\text{Zr}_{0.5}\text{O}_2$ is confirmed by *ab initio* simulation of electronic structure.

1. Introduction

Recently ferroelectricity was demonstrated in thin of the solid solution $\text{Hf}_{0.5}\text{Zr}_{0.5}\text{O}_2$ (HZO) [1–4]. Ferroelectricity in these films is associated with the ability to stabilize non-centrosymmetric orthorhombic phase $Pbc2_1$ [2]. These materials have a number of advantages over conventional ferroelectric regarding compatibility with technological processes used in microelectronics, and has already demonstrated their ability to provide very high element density. Taking into account advantages of the ferroelectric random access memory (non-volatile, high-speed performance, high number of switching cycles) the discovery of ferroelectric effect in hafnia-based materials gave an impetus for development of universal memory concept, which may lead to a significant breakthrough in the development of memory devices.

An unsolved problem in the way of development of FeRAM-based universal memory is the spontaneous depolarization of the active medium, which leads to short data storage time (retention) [5]. One of the possible reason of spontaneous depolarization is leakage currents through the ferroelectric thin films. High- κ HZO thin films ($\kappa > 16$) can be used as sub-gate dielectrics in MOSFET and FinFET transistors instead of SiO_2 . Thus, it is very important to know charge transport mechanisms in thin dielectrics films to control the leakage currents for development of high quality memory devices. Purpose of the present work is to study charge transport mechanism in ferroelectric HZO.



2. Experiment details

Transport measurements were performed for TiN/HZO/Pt structures. Test structures were fabricated with ALD technique. The TiN layer (10 nm) was deposited on oxidized Si substrate. Then the 10-nm-thick HZO films were deposited at 240 °C from TEMAHf, TEMAZr, and H₂O precursors. The thickness and stoichiometry of the films were confirmed by laser ellipsometry and Rutherford backscattering spectroscopy. A part of the samples was treated by rapid thermal annealing (RTA) at 400 °C in N₂ atmosphere. The crystalline structures of the films were examined by symmetrical X-Ray diffraction (XRD) using ARL X'TRA tool (Thermo Scientific) utilizing CuK α radiation. Top Pt electrodes were deposited through a shadow mask with round holes (area is $7.1 \times 10^4 \mu\text{m}^2$) by electron beam evaporation on HZO films.

The DC current-voltage (I - V) curves were measured using Agilent B1500A Semiconductor device parameter analyser. Polarization-voltage (P - V) curves were obtained by integration of displacement current response in reply to the stepped triangle voltage. The leakage current was subtracted from the current response in order to eliminate the polarization and displacement current contributions.

The electronic structure of HZO was calculated within the spin-polarized density functional theory using the *ab initio* simulation program package Quantum ESPRESSO with B3LYP functional. The oxygen vacancy (V_{O}) was generated by the removal of an O atom, followed by relaxation of the remaining atoms in a 96-atom supercell.

3. Results and discussions

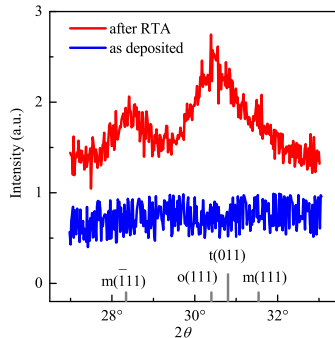


Figure 1. XRD spectra of as deposited and after RTA HZO.

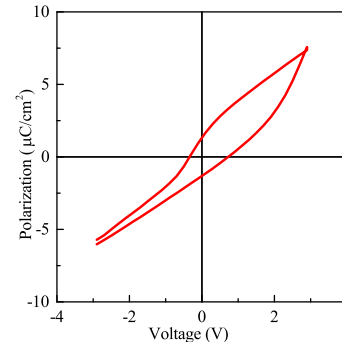


Figure 2. Polarization-voltage characteristics for TiN/f-HZO/Pt structures.

The XRD spectra of as-deposited and annealed films are presented in Fig. 1. One can see that as-deposited films have an amorphous structure (a-HZO), while annealed films are polycrystalline with monoclinic, tetragonal, and orthorhombic phases. The presence of ferroelectricity of after-RTA-films is confirmed by observing characteristic hysteresis on the P - V plot (Fig. 2).

Figure 3 shows results of *ab initio* calculations performed for four types of oxygen vacancy in orthorhombic HZO. The calculated partial density of states (PDOS) of oxygen, hafnium, and zirconium atoms for all types of neutral oxygen vacancies V_{O} in HZO are shown in Figures 4(a)–(d). The $\text{ZrZr}=\text{V}_{\text{O}}-\text{Hf}$ and $\text{HfHf}=\text{V}_{\text{O}}-\text{Zr}$ defects represent threefold oxygen vacancies with 2 Zr+Hf and 2 Hf+Zr metal atoms around, while $\text{HfHf}=\text{V}_{\text{O}}=\text{ZrZr}$ and $\text{HfZr}=\text{V}_{\text{O}}=\text{HfZr}$ defects represent fourfold oxygen vacancies with different spatial arrangements of Hf and Zr atoms around the vacancy. The schematic spatial configurations of the defects are shown in the insets of the Fig. 4(a)–(d). One can see that the electronic structures of the different-type oxygen vacancies in HZO are similar: threefold and fourfold coordinated vacancies form filled states in the band gap of 3.4 eV and 2.7 eV above the valence band, respectively. The nearest metal atoms to

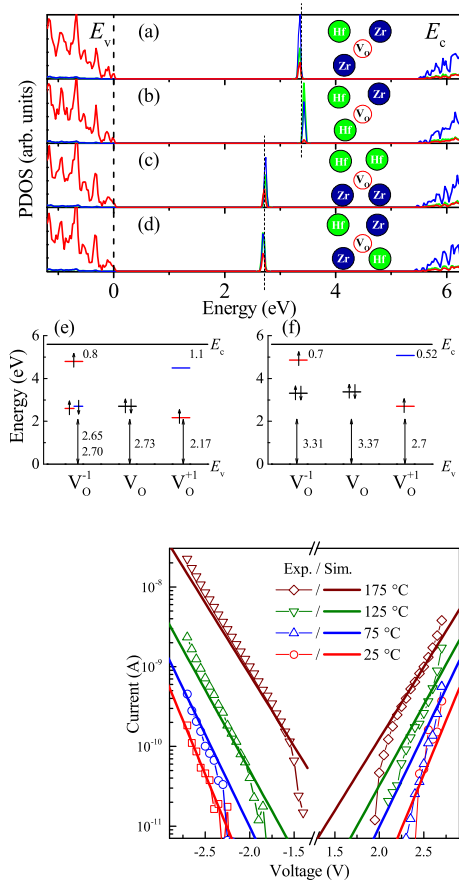


Figure 4. Experimental (characters) current-voltage characteristics and simulations (lines) for TiN/f-HZO/Pt structures at different temperatures.

the oxygen vacancy give the most contribution to the defect states as shown in Fig. 4(a)–(d). The next most important contribution to the defect state is given by the nearest to the oxygen vacancy atoms. Calculated Kohn-Sham energy levels for the oxygen vacancies in different charge states are shown in Figs. 4(e)–(f). We can see that a trapped on the defect electron has an energy of ~ 1 eV below E_c . Trapping a hole leads to a descent of the energy level compared to neutral oxygen vacancy. Thus, we conclude that the defect states in the band gap are localized, and the oxygen vacancies can act as a trap for electrons, as well as for holes, being involved in the charge transport.

Despite that *ab initio* calculations predict amphoteric nature of traps, the capacitance-voltage measurements on trapped charge accumulation demonstrate that mostly holes are involving in transport processes [6]. Thus, further analysis we will perform in terms of monopolar hole conductivity.

Figure 4 shows experimental current-voltage characteristics of leakage current contribution in f-HZO at different temperatures T on semi-log I – V – T plate. The current depends on the voltage and temperature exponentially. The Frenkel model [7], can describe experimental I – V – T dependencies using underestimated value of frequency factor. Following by [6, 8], we analysed

Figure 3. The calculated partial density of states (PDOS) of oxygen, hafnium and zirconium atoms for all types of neutral oxygen vacancy V_O in HZO: (a) $ZrZr=V_O-Hf$, (b) $HfHf=V_O-Zr$, (c) $HfHf=V_O=ZrZr$, (d) $HfZr=V_O=HfZr$. The energy levels of $HfHf=V_O=ZrZr$ -type (e) and $HfHf=V_O-Zr$ -type (f) oxygen vacancy in different charge states: V_O^{-1} is negatively charged state, V_O^{+1} is positively charged state. The spins of localized on the defect electrons are shown with arrows. The distance between energy levels and the top of the valence band (in eV) are shown by bilateral arrows. The reference point is the top of valence band E_v .

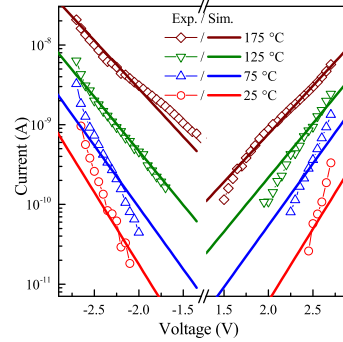


Figure 5. Experimental (characters) current-voltage characteristics and simulations (lines) for TiN/a-HZO/Pt structures at different temperatures.

experimentally measured $I-V-T$ in terms of phonon-assisted tunnelling between traps [9]:

$$J = \frac{e}{s^2} \gamma (1 - \gamma) \frac{\sqrt{2\pi\hbar W_t}}{m^* s^2 \sqrt{(W_{\text{opt}} - W_t) kT}} \exp\left(-\frac{W_{\text{opt}} - W_t}{2kT}\right) \exp\left(-\frac{2s\sqrt{2m^* W_t}}{\hbar}\right) \sinh\left(\frac{eFs}{2kT}\right), \quad (1)$$

where J is the current density, e is the elementary charge, s is mean distance between traps, γ is trap filling factor, \hbar is the Planck constant, W_t is thermal trap energy, W_{opt} is optical trap energy, m^* is the effective mass, k is the Boltzmann constant, F is the electric field in the dielectric. One can see that the current-voltage characteristics (1) exhibits a maximum at $\gamma = 0.5$. Phonon-assisted tunnelling between traps (lines on Fig. 4) describes experimental $I-V-T$ curves with very good quantitative agreement using thermal and optical trap energies $W_t = 1.25$ eV and $W_{\text{opt}} = 2.5$ eV, respectively, $m^* = 0.21m_0$ (hereby m_0 is the free electron mass), trap density $N = s^{-3} = 3 \times 10^{19} \text{ cm}^{-3}$.

The same procedure was applied for MOS structures with amorphous HZO. Figure 5 represents comparison of experimentally measured current-voltage characteristics for a-HZO at different temperatures with calculated within (1). The best agreement of calculated curves with experimental data was got with parameter values: $W_t = 1.25$ eV, $W_{\text{opt}} = 2.5$ eV, $m^* = 0.3m_0$, $N = 1 \times 10^{20} \text{ cm}^{-3}$. It should be noted that obtained values of trap energies are the same as for amorphous a-Hf_xZr_{1-x}O_y, synthesized by different techniques [6].

Since thermal and optical energies for amorphous and ferroelectric HZO films do not depend on crystal phase, one can assume that the traps in different phases of these films have the same nature. Recently it was shown that the oxygen vacancies act as the charge traps in hafnium oxide [8]. At the same time, thermal and optical trap energies in HfO₂ have the same values. Taking into account, that the oxygen vacancies in HfO₂ and ZrO₂ have the same electronic structure, the fact that HZO is the solid solution of these oxides, one can assume that the oxygen vacancies act as the charge traps in a-HZO and f-HZO. Thus, we conclude that the leakage currents mechanism in HZO does not depend on crystal structure of HZO films, and it is phonon-assisted tunnelling between oxygen vacancies. The only difference is charge trap density, which is lower in f-HZO. This difference might be caused by RTA treatment during film preparation.

4. Summary

In conclusion, we demonstrated that the charge transport of amorphous and ferroelectric HZO films is described by phonon-assisted tunnelling between traps. The thermal and optical trap energies in HZO were revealed as 1.25 eV and 2.5 eV, respectively. It was concluded that the traps are oxygen vacancies. A hypothesis that oxygen vacancies are responsible for the charge transport in HZO is confirmed by electronic structure *ab initio* simulation.

Acknowledgments

The work was supported by the Ministry of Education and Science of the Russian Federation (project #RFMEFI57614X0065) (synthesis of HZO films) and the Russian Science Foundation (project #14-19-00192) (transport measurements and simulation).

References

- [1] Müller J *et al* 2011 *Appl. Phys. Lett.* **99** 112901
- [2] Müller J *et al* 2012 *Nano Lett.* **12**(8) 4318–4323
- [3] Hyuk Park M *et al* 2013 *Appl. Phys. Lett.* **102** 112914
- [4] Chernikova A *et al* 2015 *Microelectron. Eng.* **147** 15–18
- [5] Cheng C H and Chin A 2014 *IEEE Electron Device Lett.* **35** 138–140
- [6] Islamov D R *et al* 2015 *Appl. Phys. Lett.* **106**(10) 102906 (*Preprint* 1501.02370)
- [7] Frenkel J 1938 *Tech. Phys. USSR* **5**(9) 685–695
- [8] Islamov D R, Gritsenko V A, Cheng C H and Chin A 2014 *Appl. Phys. Lett.* **105** 222901 (*Preprint* 1409.6887)
- [9] Nasyrov K A and Gritsenko V A 2011 *JETP* **112** 1026–1034 ISSN 1063-7761